



Microbial indicators of efficient performance in an anaerobic/anoxic/aerobic integrated fixed-film activated sludge (A²O-IFAS) and a two-stage mesophilic anaerobic digestion process.

P. Maza-Márquez^{a,b,1}, M.J. Gallardo-Altamirano^{a,d,*}, F. Osorio^{a,c}, C. Pozo^{a,b}, B. Rodelas^{a,b}

^a Environmental Microbiology Group, Institute of Water Research, University of Granada, C/ Ramón y Cajal, n°4, 18071, Granada, Spain

^b Department of Microbiology, University of Granada, 18071, Granada, Spain

^c Department of Civil Engineering, University of Granada, 18071, Granada, Spain

^d Department of Chemical Engineering, University of Granada, 18071, Granada, Spain

HIGHLIGHTS

- Microbial community structure was assessed in an A²O-IFAS two-stage MAD system.
- Improved N and P removals were achieved in the A²O-IFAS operating at short SRT.
- N removal was correlated with the abundance of denitrifiers in the attached biomass.
- Short SRT generated highly biodegradable WAS that favored efficient methanogenesis.
- The efficiency of methanogenesis correlated with high abundance of *Acetobacteroides*.

GRAPHICAL ABSTRACT



ARTICLE INFO

Handling Editor: A Adalberto Noyola

Keywords:

A²O

Two-stage anaerobic digestion

ABSTRACT

An analysis of the community structure, diversity and population dynamics of *Bacteria* and *Archaea* in the suspended and attached biomass fractions of a pilot-scale anaerobic/anoxic/aerobic integrated fixed-film activated sludge (A²O-IFAS) was executed. Along with this, the effluents of the acidogenic (AcD) and methanogenic (MD) digesters of a two-stage mesophilic anaerobic (MAD) system treating the primary sludge (PS) and waste activated

Abbreviations: A²O, anaerobic/anoxic/aerobic; AcD, acidogenic digester; Alk, alkalinity; AS, activated sludge; BFSS, biofilm suspended solids; BFVSS, biofilm volatile suspended solids; BOD₅, biological oxygen demand at 5 days; COD, chemical oxygen demand; DO, dissolved oxygen; F/M, food-to-microorganisms ratio; HRT, hydraulic retention time; IFAS, integrated-fixed film activated sludge; MAD, mesophilic anaerobic digestion; MBBR, moving-bed biofilm reactor; MD, methanogenic digester; MDS, Non-metric multidimensional scaling; MLSS, mixed liquor suspended solids; MLVSS, mixed liquor volatile solids suspended; NLR, nitrogen loading rate; %NRR, total N removal rate; OLR, organic loading rate; %ORR, organic removal rate; T, temperature; PAOs, polyphosphate accumulating organisms; PHY, phylotype; %PRR, total P removal rate; PS, primary sludge; qPCR, quantitative polymerase chain reaction; RA, relative abundance; RAS, % of return activated sludge; SRT, sludge retention time; SVI, sludge volumetric index; TN, total nitrogen; TP, total phosphorous; ThS, thickened sludge; TS, total solids; TSS, total suspended solids; UPGMA, unweighted pair group method with arithmetic mean; VFA, volatile fatty acids; VS, volatile solids; %VSR, volatile solid removal percentage; WAS, waste activated sludge; WWT, wastewater treatment.

* Corresponding author. Environmental Microbiology Group, Institute of Water Research, University of Granada, C/ Ramón y Cajal, n°4, 18071, Granada, Spain.

E-mail address: manujga@ugr.es (M.J. Gallardo-Altamirano).

¹ P. M.-M. and M.J. G.-A. contributed equally to this work.

<https://doi.org/10.1016/j.chemosphere.2023.139164>

Received 9 February 2023; Received in revised form 15 May 2023; Accepted 6 June 2023

Available online 7 June 2023

0045-6535/© 2023 The Authors. Published by Elsevier Ltd. This is an open access article under the CC BY-NC license (<http://creativecommons.org/licenses/by-nc/4.0/>).

Nutrient removal
Microbial diversity
Microbial indicators

sludge (WAS) generated by the A²O-IFAS were also analyzed. Non-metric multidimensional scaling (MDS) and Biota-environment (BIO-ENV) multivariate analyses were performed to link population dynamics of *Bacteria* and *Archaea* to operating parameters and removal efficiencies of organic matter and nutrients, in search of microbial indicators associated with optimal performance. In all samples analyzed, *Proteobacteria*, *Bacteroidetes* and *Chloroflexi* were the most abundant phyla, while the hydrogenotrophic methanogens *Methanolinea*, *Methanocorpusculum* and *Methanobacterium* were the predominant archaeal genera. BIO-ENV analysis disclosed strong correlations between the population shifts observed in the suspended and attached bacterial communities of the A²O-IFAS and the removal rates of organic matter, N and P. It is noteworthy that the incorporation of carriers combined with a short sludge retention time (SRT = 4.0 ± 1.0 days) enhanced N removal performance of the A²O by favoring the enrichment of bacterial genera able to denitrify (*Bosea*, *Dechloromonas*, *Devosia*, *Hyphomicrobium*, *Rhodobacter*, *Rhodoplanes*, *Rubrivivax*, and *Sulfuritalea*) in the attached biomass fraction. In addition, operation at short SRT enabled the generation of a highly biodegradable WAS, which enhanced the biogas and methane yields in the two-stage MAD. An increase in the relative abundance of *Acetobacteroides* (uncultured Blvii28 wastewater-sludge group of *Rikenellaceae* family) correlated positively with the volatile solids removal rate (%VSR), CH₄ recovery rate and %CH₄ in the biogas (r > 0.8), supporting their relevance for an efficient methanogenesis in two-stage systems.

1. Introduction

The development of wastewater treatment (WWT) technologies currently faces the challenge to provide an efficient removal of organic matter, N and P, in order to meet the growing demands of the discharge regulation standards, while minimizing sludge production and keeping a reduced operating cost. Among the different enhanced biological nutrient removal technologies available, the single-sludge suspended-growth system comprising sequential anaerobic, anoxic, and aerobic stages (A²O) is the most widely used (Raj et al., 2013). This process brings about several advantages including easy and stable operation, low energy requirements, cost-effectiveness, improved sludge settling, maintenance of an adequate alkalinity in the aerobic reactor for nitrification, and high N removal rates (Demir, 2020; Gallardo-Altamirano et al., 2018). However, in A²O systems, low or unstable performance of N and P removal may occur, due to competition for carbon substrates and electron acceptors among functional microbial groups with different optimal settings of operational parameters, like sludge retention time (SRT) or dissolved oxygen (DO) concentration (Wang et al., 2006; Zhao and Bai, 2022).

A simple and low-cost upgrade of the conventional A²O is the integrated-fixed film activated sludge (IFAS) configuration, consisting of the incorporation of carriers as support for the development of microbial biofilms. This technology combines suspended growth biomass in the circulating mixed liquor, and carrier-attached biomass that remains retained in the bioreactors (Onnis-Hayden et al., 2011; Rosso et al., 2011). In biofilms, cell assemblages surrounded by a self-generated polymeric matrix bind to the carriers' surface into a three-dimensional structure with spatial heterogeneity, and gradients of substrates and DO cause stratification of the biofilm into different zones favoring the coexistence of physiologically diverse microbial groups and the cooperation among them (Jo et al., 2022). The biofilm lifestyle enhances the proliferation of slow-growing populations, provides a better environmental resilience, promotes horizontal gene transfer, and facilitates the removal of recalcitrant molecules (Verma et al., 2022). Consequently, the IFAS configuration increases the treatment capacity of the conventional suspended growth systems, allowing for higher loading rates, offering further flexibility of operation at varying hydraulic retention times (HRT), and reducing sludge production (Rosso et al., 2011).

The diversity of the microbial communities has been explored in a number of WWT technologies combining suspended and attached growth phases, including A²O-IFAS systems (Aqeel and Liss, 2022; Phanwilai et al., 2020; Wang et al., 2021a; Zhao and Bai, 2022). Prokaryotic populations, and particularly functional microbial groups, respond to environmental and operational variables and impact process performance, thus serving as bioindicators of both process stability and efficiency in engineered systems (Carballa et al., 2015; Urakawa and Bernhard, 2017). Even though such knowledge can significantly aid for a

further optimization of the design and operation of enhanced biological nutrient removal processes, the links among the changes of community structure derived from the implementation of the IFAS configuration and the improvement of WWT efficiency have been seldom explored.

In previous studies, we described the upgraded performance of a pilot-scale A²O-IFAS versus its conventional configuration (Gallardo-Altamirano et al., 2018, 2019, 2021b). The main purpose of the present study was to carry out an analysis of the community structure and population dynamics of *Bacteria* and *Archaea* in the suspended and attached biomass fractions of the pilot-scale A²O-IFAS, seeking for correlations among the shifts of the relative abundance of specific taxa and the removal rates of organic matter, N and P. In addition, the performance and community diversity in the acidogenic and methanogenic digesters of a two-stage mesophilic anaerobic digestion (MAD) process designed to treat the primary sludge (PS) and waste activated sludge (WAS) generated by the A²O-IFAS were also monitored.

2. Material and methods

2.1. Description of the wastewater treatment pilot-scale plant

The pilot-scale plant used in this study (Fig. 1) was sited at the facilities of the WWT plant *Murcia Este* (EMUASA, Murcia, Spain). The A²O-IFAS bioreactor was fed with wastewater taken from the pre-treatment of the adjacent full-scale municipal plant. The aerated bioreactor (1.20 m³), which was split into four chambers (C1, C2, C3 and C4), was filled at 50% with AnoxKaldnes K5 (Veolia AnoxKaldnes®) carriers to achieve 0.36 filling ratio of the total bioreactor volume (1.66 m³). The characteristics of the carriers have been previously described by Gallardo-Altamirano et al. (2021b).

The start-up and the stabilization phase of the A²O-IFAS lasted from 2nd May to August 2, 2017. After the steady state was reached, the experimental phase was developed for 105 days (3rd August 2017–15th November 2017). In the two-stage MAD, the acidogenic and methanogenic digesters (AcD and MD, respectively) treated the thickened sludge (ThS) produced by the A²O-IFAS throughout its start-up and stabilization, operating with the same SRTs (2 and 12 days, respectively). Since July 1, 2017, the A²O-IFAS worked under steady-state conditions producing a regularly ThS at a volatile solid flow of 795 ± 181 L d⁻¹ (Gallardo-Altamirano et al. (2021b)). Thereby, the digesters started up operating at a constant organic loading rate (OLR) during 31 days before the experimental phase started.

Both the A²O-IFAS and the two-stage MAD were equipped with a supervisory control and data acquisition (SCADA) system to control the operational parameters. A full description of the pilot plant is available elsewhere (Gallardo-Altamirano et al., 2021a, 2021b).

2.2. Physicochemical parameters and monitoring of the A²O-IFAS two-stage MAD plant performance

Throughout the experimental phase, 24-h composite samples were taken from the influent, decanted influent and effluent of the A²O-IFAS (sampling points 1, 2 and 3, respectively, Fig. 1) three times per week to measure the following parameters: chemical oxygen demand (COD), biological oxygen demand at 5 days (BOD₅), total suspended solids (TSS), total P (TP), total N (TN), N-NH₄⁺, N-NO₃⁻, pH, OLR, nitrogen loading rate (NLR), phosphorus loading rate, (PLR), and the removal rates of organic matter (%ORR), nitrogen (%NRR), phosphorus (%PRR) and suspended solids. The operating temperature (T), DO, F/M, sludge volumetric index (SVI), MLSS, mixed liquor volatile suspended solids (MLVSS), biofilm suspended solids (BFSS), and biofilm volatile suspended solids (BFVSS) were also periodically monitored in sludge and/or biofilm samples. Monthly average data (\pm standard deviation) of all the aforementioned variables and full methodologies are described in detail in Gallardo-Altamirano et al. (2021b).

Since the stabilization phase (01/07/2017–01/08/2017) and throughout the steady-state, the A²O-IFAS operated with concentrations of MLSS and BFSS ranging 1500–2000 mg L⁻¹ and 1000–2000 mg L⁻¹, respectively. The mixed liquor SRT was maintained between 3.5 and 4.5 days, and the mixed liquor food-to-microorganism ratio (F/M) was kept over 0.40 kg BOD₅ kg⁻¹ MLVSS d⁻¹.

In the two-stage MAD plant, temperature, pH, biogas production and biogas composition were recorded daily in both digesters. In order to evaluate the performance of the anaerobic digestion, total solids (TS), volatile solids (VS), volatile fatty acids (VFA) and alkalinity (Alk) were analyzed in sludge samples taken three times a week from three different sampling points: ThS and effluents of the AcD and MD (4, 5 and 6 in Fig. 1, respectively). The methodology for the analytical determinations is described in Gallardo-Altamirano et al. (2021a).

2.3. DNA extraction, qPCR, massive parallel sequencing, and data analysis

Biomass samples were retrieved from the pilot-scale plant as follows.

Activated sludge (AS) and carriers holding biofilms were collected from the aerated bioreactor of the A²O-IFAS to sample the suspended and attached biomass, respectively. Carriers were collected separately from both the first and fourth of the four compartments of the aerated bioreactor (C1 and C4, respectively, Fig. 1), while composite samples of AS from the 4 chambers were taken. Sludge was retrieved from the effluents of the AcD and MD of the two-stage MAD (sampling points 5 and 6, Fig. 1). Henceforth, the five types of samples will be named AS, C1, C4, AcD and MD, respectively. Samples were retrieved monthly throughout the experimental period (August 02, 2017, September 07, 2017, October 11, 2017 and November 15, 2017).

The biomass in the AS, AcD and MD samples (4 mL, 3 replicates) was pelleted by centrifugation (14 000×g, 1 min). C1 and C4 samples consisted of two carrier units retrieved from each compartment with the aid of a sterile sieve-sampling device, from which the attached biomass was removed following the procedures described by Reboleiro-Rivas et al. (2016). Briefly, carriers in each sample were placed in flasks with 50 mL sterile saline (0.9% NaCl), vortexed for 1 min, and sonicated in a bath at room temperature for 3 min at 53 kHz. The resultant biofilm suspensions were pelleted by centrifugation (3000×g, 5 min). The full procedure was repeated twice. Environmental DNA was extracted from all biomass samples using the FastDNA-2 mL SPIN kit for Soil and the FastPrep24 apparatus (MP-Bio, Santa Ana, CA, USA) as described by Gallardo-Altamirano et al. (2018), and stored at -20 °C.

Real-time quantitative PCR (qPCR) of partial 16 S rRNA genes was used to measure the absolute abundances of *Bacteria* and *Archaea* populations in the biomass samples, using a QuantStudio-3 Real Time PCR system (Applied Biosystems, Waltham, MA, USA). The primer pairs used, reactions and cycling conditions were previously described in detail by Gallardo-Altamirano et al. (2018). The results were expressed per L of bioreactor volume, as previously described by Reboleiro-Rivas et al. (2016).

High-throughput Illumina MiSeq sequencing (Illumina, Hayward, CA, USA) of the 16 S rRNA genes was done at the facilities of RTL Genomics (Lubbock, TX, USA, <http://www.researchandtesting.com>), using primer pairs 28 F–519 R (Fan et al., 2012) and 517 F/909 R (Maspolim et al., 2015) for *Bacteria* and *Archaea*, respectively. Raw sequencing data

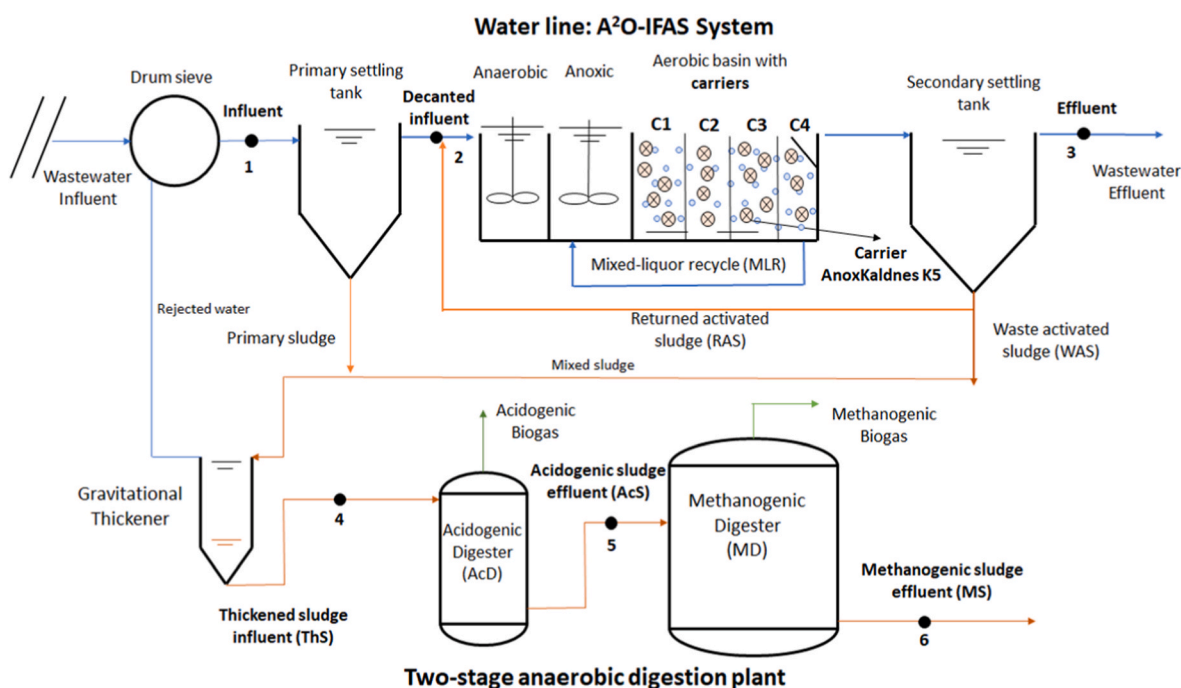


Fig. 1. Schematic diagram of the pilot-scale anaerobic/anoxic/aerobic integrated fixed-film activated sludge and two-stage mesophilic anaerobic digestion plant (A²O-IFAS two-stage MAD).

were processed using the QIIME software, v. 1.9.1 (Caporaso et al., 2012), as described elsewhere (Gallardo-Altamirano et al., 2019, 2021a). Taxonomic close-reference assignments based on 97% sequence identity were done using the Greengenes database (version 13_08).

The PAST v. 3.25 software (Hammer et al., 2001) and the iNEXT online tool (<https://chao.shinyapps.io/iNEXTOnline>, Hsieh et al., 2016) were used to calculate Alpha-diversity indices and render sample-size-based rarefaction and extrapolation (R/E) curves, respectively. Generation of UPGMA (unweighted pair group method with arithmetic mean) dendrograms and evaluation of the contribution of individual phylotypes (PHYs) to the (dis)similarity among clusters of samples were achieved with the SIMPROF and SIMPER tools, respectively, provided by the Primer software (PRIMER-E v. 6.1.18, Plymouth, UK). Heatmaps showing the relative abundances (RAs) of *Bacteria* and *Archaea* populations in the sets of samples were constructed with Microsoft Excel.

2.4. Statistical analyses

The Kruskal-Wallis and Conover-Iman tests were conducted to look for significant differences ($p < 0.05$) among the different types of samples. IBM SPSS Statistics v. 19 (SPSS Inc., IBM, USA) and the R software (<http://www.rproject.org/>) were used to conduct these statistical tests. Multivariate statistical analyses (Analysis of similarity, ANOSIM; non-metric multidimensional scaling, MDS; and biota-environment analysis, BIOENV) were completed with the aid of the Primer software (PRIMER-E v. 6.1.18, Plymouth, UK), following the methods previously described by Maza-Márquez et al. (2016).

3. RESULTS and DISCUSSION

3.1. Performance of the pilot-scale plant for organic matter and nutrients' removal

As already stated in the Introduction, the performance of the A²O-IFAS for the removal of organic matter and nutrients from municipal wastewater was analyzed in a previous study (Gallardo-Altamirano et al., 2021b) and the most relevant parameters are summarized in Table S1. In brief, the A²O-IFAS configuration allowed significantly higher average removals of N and P than the conventional A²O process (%NRR = 72.8, 28% and 8% higher than in phases I and II, respectively; %PRR = 75.0, 53% and 13% higher than in phases I and II, respectively), even though it was operated at shorter mixed liquor SRT, lower mixed liquor suspended solids (MLSS) concentrations, and lower COD/TN ratio (Table S1).

Tables S2–S4 display the comparisons among the operational conditions and performance of the AcD, MD and the global two-stage MAD when the PS and WAS from either the conventional A²O system (phases I and II, Gallardo-Altamirano et al., 2021a) or the A²O-IFAS (phase III, this study) were treated. Table S5 summarizes the characterization of the ThS, AcD and MD effluents in the three experimental phases.

The AcD and MD were set to operate under mesophilic conditions at 35 °C. However, an exception occurred during phase III, when the AcD temperature was 35 °C for the first 60 days of operation but decreased gradually from 35 to 30 °C throughout the next 47 days. This temperature shift did not influence the CH₄ yield of the AcD or the global two-stage MAD. In this sense, Chae et al. (2008) reported a CH₄ yield reduction of only 3% in an anaerobic digester operated at 30 °C compared to 35 °C.

The average total solids percentage in the ThS (2.31 ± 0.43 %TS) and the global OLR applied to the two-stage MAD in phase III (1.6 ± 0.4 Kg VS m⁻³ d⁻¹) were lower compared with a high-rate AD process for sewage sludge (Appels et al., 2008; Metcalf and Eddy, 2003; Ponsá et al., 2008). A similar trend occurred in phases I and II, when the two-stage MAD treated the sludge coming from the conventional A²O system (Table S5). Normally, for a high-rate AD process, the OLR should be

between 1.6 and 4.8 Kg VS m⁻³ d⁻¹ with a sludge concentration between 4 and 7%. It is known that operating at low OLR and low %TS decreases the efficiency of the AD process (Appels et al., 2008; Xu et al., 2020).

The water line produced a similar mass flow (TS flow of ThS) in the three experimental phases (Table S5). However, the contribution of WAS to the ThS was significantly higher in phase III ($70 \pm 11\%$ vs. 33 ± 15 and $43 \pm 16\%$, Table S2). The observed difference was because the A²O-IFAS system operated at shorter mixed liquor SRT (Table S1), which produces a higher mass flow of WAS with a higher volatile biomass percentage (%MLVSS 84% vs. 79%, Table S1). Generally, when WWT plants operate under such conditions, the biodegradability of the WAS and the biogas production in the AD process are increased (Bolzonella et al., 2005; Gonzalez et al., 2018; Xu et al., 2020).

In this sense, the global volatile solid removal percentage (%VSR) reported for the two-stage MAD treating WAS produced by the A²O-IFAS system (phase III) was significantly higher than in phase I operated at a similar SRT (14 days), and still slightly higher than in phase II when the SRT was double (29 days) ($54.3 \pm 12.1\%$ vs. $32.8 \pm 8\%$ and $50.5 \pm 14.6\%$, respectively). Consequently, the methane production, the biogas production rate and the biogas and methane yields obtained by the global two-stage MAD, and particularly in the MD, were significantly higher when the sludge came from the A₂O-IFAS (Tables S3 and S4). In the literature, the typical values reported for %VSR of WAS are often less than 35% in single-stage mesophilic digesters operating at SRTs of 20–30 days (Gonzalez et al., 2018; Parkin and Owen, 1986; Xu et al., 2020). For instance, Bolzonella et al. (2005) reported a %VSR between 15 and 27% in five full-scale single-stage digesters with SRTs ranging 20–40 days, treating WAS coming from biological nutrient removal WWT plants. These authors found a clear relationship between the methane yield production and the SRT applied in the activated-sludge process of the WWT plants: the longer the SRT, the lower the methane yield production.

3.2. Quantification of Bacteria and Archaea in the A²O-IFAS-two-stage MAD plant

Table 1 shows the numbers of copies of gene markers of *Bacteria* and *Archaea* in the biomass retrieved from AS, C1, C4, AcD and MD in the pilot-scale plant. The Conover-Iman test detected significant differences for both prokaryotic groups among all the sampling points. The average numbers of 16 S rRNA copies L⁻¹ of sludge of both *Bacteria* and *Archaea* were significantly higher in the two-stage MAD samples compared to the A²O-IFAS samples. The absolute abundance of *Bacteria* ranged between 10¹⁰–10¹¹ copies 16 S rRNA gene L⁻¹, and the quantifications in C1, AcD and MD were up to one order of magnitude higher than in the AS and C4 samples. In this sense, the biofilms on the carriers were visibly thicker in the C1 chamber compared to C4 in all samplings (Fig. S1), and the average BFSS values were nearly two-fold (Table S1). *Archaea* gene markers ranged 10⁸–10¹⁰ copies 16 S rRNA genes L⁻¹, with AcD and MD carrying significantly higher numbers of *Archaea* (ca. two orders of magnitude) over those measured in the 3 types of samples of the A²O-

Table 1

Average numbers of copies \pm standard deviations of Bacteria and Archaea gene markers (16 S rRNA gene copies/L sludge) in the different samples retrieved from the pilot-scale plant: suspended biomass in the activated sludge (AS), attached biomass in C1 and C4 carriers of the A²O-IFAS, and effluents of the acidogenic and methanogenic digesters (AcD and MD) of the two-stage MAD system. Values marked with the same letter do not significantly differ, according to the Kruskal-Wallis and Conover Iman tests.

Sample type	Bacteria	Archaea
AS	$1.16 \cdot 10^{10} \pm 7.78 \cdot 10^9$ ^a	$3.57 \cdot 10^8 \pm 1.55 \cdot 10^8$ ^a
C1	$1.02 \cdot 10^{11} \pm 1.99 \cdot 10^{11}$ ^b	$5.69 \cdot 10^8 \pm 2.68 \cdot 10^8$ ^b
C4	$6.21 \cdot 10^{10} \pm 9.10 \cdot 10^{10}$ ^b	$7.28 \cdot 10^8 \pm 9.31 \cdot 10^7$ ^c
AcD	$2.59 \cdot 10^{11} \pm 3.33 \cdot 10^{11}$ ^c	$2.33 \cdot 10^{10} \pm 1.47 \cdot 10^{10}$ ^d
MD	$3.74 \cdot 10^{11} \pm 4.19 \cdot 10^{11}$ ^c	$5.44 \cdot 10^{10} \pm 4.32 \cdot 10^{10}$ ^e

IFAS.

Overall, comparing the results of the present study with those of previous experiments conducted in the same pilot-scale plant lacking the attached growth configuration in the A²O, the absolute abundances of *Bacteria* and *Archaea* in the suspended biomass of the aerated bioreactor fell within the same range, while in the AcD and MD effluents of the two-stage MAD the numbers of gene markers (16 S rRNA genes) of both prokaryotic groups calculated using qPCR were 2–3 logarithmic units higher (Gallardo-Altamirano et al. 2018, 2021a). Such increases of abundance indicated an enhanced growth of prokaryotic populations, in connection with the higher biodegradability of the WAS generated in the A²O-IFAS compared to that coming from the conventional A²O process, and led to the subsequent improvement of the biogas production rate and methane production yield in the two-stage MAD (Tables S3 and S4), as discussed in section 3.1.

3.3. Structure of bacterial and archaeal communities in the A²O-IFAS-two-stage MAD plant

The diversity of *Bacteria* and *Archaea* was investigated in the AS, C1, C4, AcD and MD samples by massive parallel sequencing of partial 16 S rRNA genes. 186 904 and 75 245 16 S rRNA quality reads were kept for *Bacteria* and *Archaea*, respectively, after filtering of the raw data (5294–15,014 sequence reads per sample for *Bacteria*, and 357–8523 for *Archaea*). The sequencing depth attained sufficed to accurately assess the diversity of both groups of prokaryotes in all the samples, according to the R/E curves shown in Fig. S2. Applying a 97% sequence identity cut-off, a total of 1428 *Bacteria* phylotypes (PHYs) and 84 *Archaea* PHYs were identified, with the numbers of PHYs per sample ranging 374–709 and 27–50, respectively.

The numbers of reads of *Bacteria* and *Archaea* in the five types of samples, as well as the average values of Richness (S), Shannon-Wiener (*H'*), Simpson's (1-D), and Chao-1 indices of diversity, are displayed in Table S6. Overall, the average values of S, *H'* and 1-D indices defined *Bacteria* communities with medium-to-high species diversity and low functional organization, while the *Archaea* communities had much lower diversity and evenness, particularly in the AcD samples. These patterns are consistent with the observations of previous studies (Gallardo-Altamirano et al., 2019, 2021a). In the case of *Bacteria*, the values of *H'* were significantly higher in the C1 and C4 samples compared to AS, meaning that the biomass attached to carriers was more diverse than the suspended growth fraction. Differences of both the community structure and functionality among the suspended and attached biomass fractions are often reported in IFAS and moving-bed biofilm reactors (MBBR). Several previous studies also concluded that the biofilms were composed of more diverse communities than the activated sludge flocs (Aqeel and Liss, 2022; Phanwilai et al., 2020; Wang et al., 2021a), while other authors did not find significant differences (Reboleiro-Rivas et al., 2016). All the aforementioned studies operated at SRT longer than set up here (>5 d).

ANOSIM analyses showed that there were significant differences of the community profiles of *Bacteria* and *Archaea* (based on the relative abundances of PHYs detected by Illumina sequencing) among the five sample types ($R = 0.90$, $p < 0.001$, and $R = 0.45$, $p < 0.002$, for *Bacteria* and *Archaea*, respectively). The clustering of the samples based on the dis(similarity) of their bacterial and archaeal communities is depicted in the dendrograms in Fig. S3. The similarity of *Bacteria* communities among the A²O-IFAS and two-stage MAD samples was <40%. The samples of suspended and attached biomass in the aerated bioreactor and the samples of the two digesters significantly clustered apart, according to SIMPROF analysis. The *Archaea* communities in the A²O-IFAS and two-stage MAD samples also clustered separately, although their structure was more conserved (>50% similarity) than in *Bacteria* communities.

3.3.1. Diversity of bacteria communities

Bacterial PHYs in the AS, C1, C4, AcD and MD samples were classified in 36 different phyla, of which only 10 were shared by all samples. The heatmap in Fig. 2 displays the 13 phyla that reached a RA $\geq 0.5\%$ in at least one sample, with *Proteobacteria*, *Bacteroidetes*, and *Chloroflexi* always cumulatively comprising >80% of the community.

In the A²O-IFAS, *Proteobacteria* and *Bacteroidetes* codominated in the suspended biomass in the initial sampling (August 02, 2017, RAs 43.80% and 44.17%, respectively), but *Proteobacteria* tended to increase and displace *Bacteroidetes* throughout the experimental period (November 15, 2017, RAs 79.39% and 15.09%, respectively). In the AcD and MD, a similar trend of populations' succession was observed for these two major phyla. *Chloroflexi* were more abundant in the attached biomass, particularly in the C4 samples, where they equaled or even surpassed the RA of *Bacteroidetes*, an also tended to reduce their RA through time, in all the biomass fractions analyzed.

Among the remaining most abundant phyla (displayed in Fig. 2), *Acidobacteria*, *Chlorobi*, *Firmicutes*, *Planctomycetes*, *Ca. Absconditabacteria* (SR1) and *Ca. Saccharibacteria* (TM7) were detected in most of the A²O-IFAS samples, often at RAs >1%. *Nitrospirae*, which are key organisms for nitrogen removal in most WWTPs (Rodelas, 2021), were found in low RA (<0.1%) except in the C4 samples (RA up to 0.87%). In the two-stage MAD, *Firmicutes* were the fourth most abundant phylum (RAs 2.34–6.93%), and *Actinobacteria*, *Planctomycetes*, *Spirochaetes*, *Synergistetes* and *Thermotogae* were detected in all samples.

Differences of the community composition among the five types of samples were also detected at the class, order (Fig. 2), and family levels (Fig. S4), with 18, 30 and 31 taxa shared by all samples, respectively. The predominant taxa (average RA > 5%) in the A²O-IFAS were *Betaproteobacteria* (32.33%), *Alphaproteobacteria* (16.71%), *Cytophagia* (12.59%), *Gammaproteobacteria* (11.68%), and *Anaerolineae* (9.95%) at the class level; *Burkholderiales* (21.94%), *Cytophagales* (12.59%), *Caldilineales* (8.96%), *Xanthomonadales* (7.68%), and *Hyphomicrobiales* (6.62%) at the order level, and *Comamonadaceae* (18.48%), *Cytophagaceae* (12.59%), *Caldilineaceae* (8.96%), and *Xanthomonadaceae* (7.24%) at the family level.

In the two-stage MAD, the community was dominated by *Bacteroidia* (36.19%), *Betaproteobacteria* (16.99%), *Alphaproteobacteria* (12.09%), *Gammaproteobacteria* (11.77%), and *Anaerolineae* (6.44%) at the class level; *Bacteroidales* (36.19%), *Burkholderiales* (12.56%), *Xanthomonadales* (7.35%), and *Rhodobacterales* (6.15%) at the order level, and *Rikenellaceae* (28.68%), *Comamonadaceae* (8.83%), and *Rhodobacteraceae* (6.14%) at the family level. The relative abundances of *Comamonadaceae* were higher in the AcD samples, while *Rikenellaceae* dominated in the MD.

390 PHYs could be identified up to the genus level, accounting for 12.5–28.1% of bacterial reads retrieved from the A²O IFAS and 39.4–69.1% from the two stage MAD, depending on the sample. Fig. S5 shows the heatmap of the 22 identified genera which reached $\geq 0.5\%$ RA in at least one sample. Only 6 genera reached RAs >3% in at least one sample in the A²O-IFAS, being *Rhodobacter* (0.77–7.50%, average 2.60%), *Caldilinea* (0.16–5.60%, average 2.26%) and *Ca. Accumulibacter* (0.25–6.05%, average 1.68%) the three most abundant. In contrast, in the two-stage MAD a single genus (*Acetobacteroides*, Blvii28 wastewater-sludge group) dominated in all samples in both the AcD (8.32–24.44%, average 15.78%) and the MD (34.63–54.18%, average 41.55%).

In order to evaluate which PHYs contributed most to the dis(similarity) of the bacterial communities in the five groups of samples, SIMPER analyses were carried out (Tables S7 and S8). Between 3 and 5 PHYs were required to cumulatively contribute at least 5% of the pairwise dissimilarities among the five types of samples (Table S8). PHY0002 (*Burkholderiales*) and PHY0005 (*Caldilineaceae*) explained the dissimilarities among the suspended and attached biomass communities in the A²O-IFAS (AS vs. C1 and AS vs. C4, 2.20% and 2.93% cumulative contribution, respectively). The AcD and MD samples were

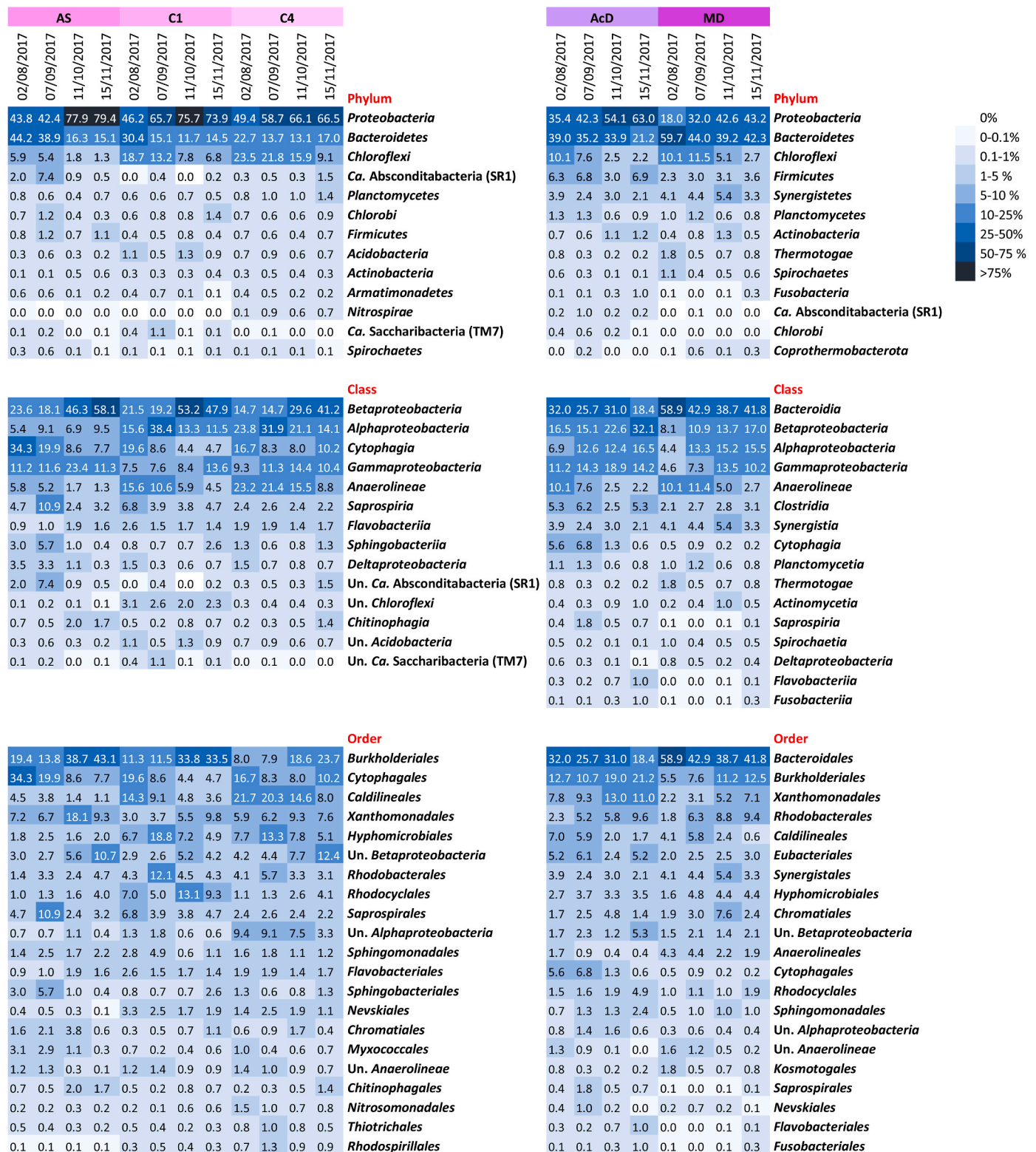


Fig. 2. Heatmap displaying the relative abundances of *Bacteria* phylotypes (Phylum, Class, and Order levels), detected by Illumina sequencing in the different samples retrieved from the pilot-scale plant: suspended biomass in the activated sludge (AS), attached biomass in the anaerobic/anoxic/aerobic integrated fixed-film activated sludge (A²O-IFAS), and effluents of the acidogenic and methanogenic digesters (AcD and MD) of the two-stage mesophilic anaerobic digestion (MAD) system. Taxa were included in the heatmaps according to the following cut-offs of relative abundance in at least one sample: Phylum $\geq 0.5\%$; Class and Order $\geq 1\%$. Un.: unclassified.

52.68–66.36% dissimilar to the A₂O-IFAS samples, with PHY001 (*Acetobacteroides* Blvii28) always contributing 2.09–4.00% to such differences.

Proteobacteria, *Bacteroidetes* and *Chloroflexi* are commonly the dominant phyla in the bacterial communities of conventional activated sludge processes and mesophilic anaerobic digesters (Ferrera and Sánchez, 2016; Xia et al., 2018). Their prevalence has also been well documented in IFAS systems by several studies based on cultivation-independent methods (Kwon et al., 2010; Wang et al., 2021a; Wu et al., 2017; Xiao et al., 2016; Yang et al., 2014; Zhao and Bai, 2022). In previous studies, when the same pilot-scale A²O was operated with suspended growth only and using a much longer SRT (12–13 d) (Gallardo-Altamirano et al., 2018, 2019), *Proteobacteria* and *Bacteroidetes* also dominated the community, although *Proteobacteria* always displayed a significantly higher RA than *Bacteroidetes* (at least two-fold) throughout operation. This difference suggests that the incorporation of carriers and development of attached biomass influenced the patterns of populations' succession in the A²O. In this sense, Aqeel and Liss (2022) reported that the biomass detached from the carriers during biofilm

dispersion was incorporated to the suspended growth fraction, significantly influencing the community dynamics of both *Proteobacteria* and *Bacteroidetes* in a laboratory-scale IFAS-sequencing batch reactor.

3.3.2. Diversity of archaea communities

Over 98% of the archaeal sequence reads identified were classified within the Phylum *Euryarchaeota* in all the analyzed samples, while the remaining reads belonged to *Thaumarchaeota* (0.0–1.8%) and *Crenarchaeota* (0.0–0.1%). *Methanomicrobia* and *Methanobacteria* were the most abundant classes in both the A²O-IFAS (average RAs 68.46 and 30.96%, respectively) and the two-stage MAD samples (average RAs 59.93 and 39.69%, respectively). The RAs of the archaeal PHYs clustered at the order, family, and genus levels in the AS, C1, C4, AcD and MD samples are shown in the heatmaps of Fig. 3. Genera of hydrogenotrophic methanogens prevailed in both the A²O-IFAS and the two-stage MAD. On average, *Methanomicrobiales* and *Methanobacteriales* dominated in the five sample types, although their RAs widely varied between sampling dates, particularly in the two-stage MAD (Fig. 3). *Methanolinea* reached the highest RAs in most of the AS, C1 and C4

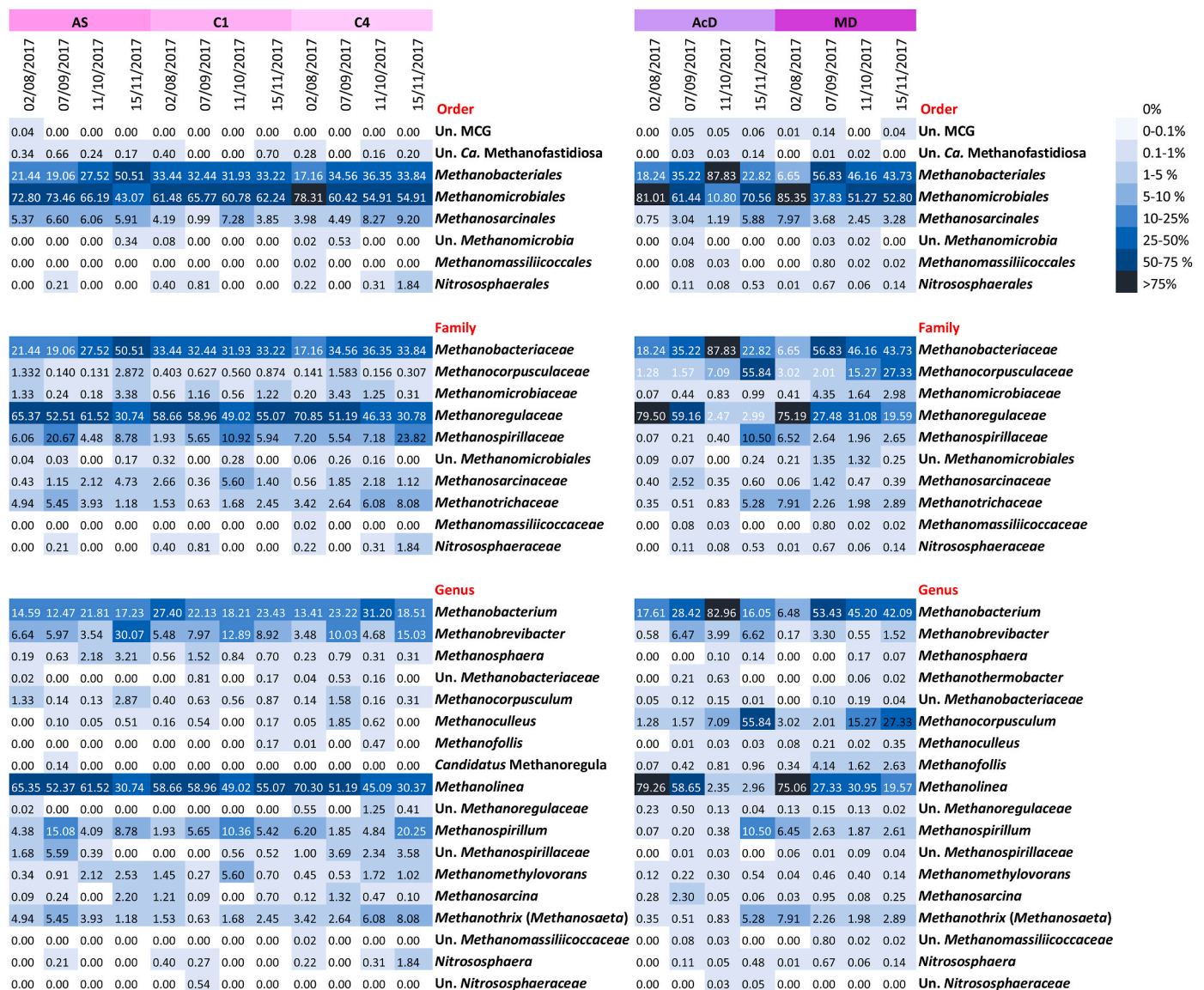


Fig. 3. Heatmaps displaying the relative abundances of Archaea phylotypes (Order, Family and Genus levels), detected by Illumina sequencing in the different samples retrieved from the pilot-scale plant: suspended biomass in the activated sludge (AS), attached biomass in C1 and C4 carriers of the anaerobic/anoxic/aerobic integrated fixed-film activated sludge (A²O-IFAS), and effluents of the acidogenic and methanogenic digesters (AcD and MD) of the two-stage mesophilic anaerobic digestion (MAD) system. Un.: unclassified. MCG: miscellaneous crenarchaeota group.

samples (30.37–70.30%), while in the AcD and MD, *Methanolinea*, *Methanocorpusculum* and *Methanobacterium* alternatively dominated throughout the experiment (2.35–79.20%, 1.28–55.84%, and 6.48–82.98%, respectively). The specialized acetotrophic and methylo-trophic methanogens (*Methanotrix* and *Methanomethylovorans*, respectively) were on average more abundant in the A²O-IFAS than in the two-stage MAD (Fig. 3). Some archaeal genera became particularly enriched in the C4 samples, including *Methanotrix* and the ammonia oxidizing archaea *Nitrososphaera*, which followed the same trends that their bacterial nitrifying counterparts (*Nitrosomonadaceae* and *Nitrospira*) (Fig. 3).

The SIMPER analyses (Table S9) calculated a global similarity >68% among the samples retrieved from either the AS, C1, C4, or MD, and >55% between those taken from the AcD. PHY001 (*Methanolinea*) always had a major contribution (12.94%–26.21%) to the similarity among samples of the same type. PHY001 and PHY002 (*Methanobacterium*) cumulatively explained >30% similarity in the AS, C1 and C4 sample groups, while in the two-stage MAD, PHY003 and PHY007 (*Methanobacterium*) together with PHY001 contributed >40% to the similarity among samples. The archaeal communities were not highly dissimilar (<32%) when comparing the suspended and attached biomass fractions in the aerated bioreactor of the A²O-IFAS (Table S10). PHY004 (*Methanolinea*) and PHY005 (*Methanobrevibacter*) contributed always to the pairwise dissimilarities among the AS, C1 and C4 samples, while PHY001, PHY003, and PHY006 (*Methanocorpusculum*) altogether explained >18% of all the pairwise dissimilarities of the archaeal communities between the A²O-IFAS and the two-stage MAD samples, and 27.9% of the dissimilarity among AcD and MD samples (Table S10).

3.4. Linking the population dynamics of bacteria to the operational parameters and performance in the A²O-IFAS

In order to further investigate the shifts of the bacterial community structure and their connections with the changes of the operating parameters and the removal efficiencies of organic matter and nutrients in the A²O-IFAS, MDS and BIOENV multivariate analyses were carried out. The MDS ordinations of the AS, C1 and C4 samples were very similar when they were based on the RAs of the PHYs clustered at the phyla, class, order or family levels. Fig. 4 shows the ordinations at the order, family and genus levels, and ordination at the class level is displayed in Fig. S6.

The prevalent orders *Burkholderiales* and *Xanthomonadales*, plus a group of uncultured *Betaproteobacteria*, consistently tended to increase their RAs in the A²O-IFAS towards the end of the experiment, regardless of the type of samples analyzed (Figs. 2 and 4A). Three of the families displaying the highest RAs (*Comamonadaceae*, *Cytophagaceae* and *Xanthomonadaceae*) showed a trend to be more abundant in the suspended growth samples (Fig. 4B), although they succeeded each other throughout the experimental time. As such, *Cytophagaceae* (*Bacteroidetes*) dominated in the AS samples in August/September 2017 (19.94–34.30%), while *Comamonadaceae* (*Burkholderiales*) dominated in all sample types (20.34–35.85%) in November 2017 (Fig. S4). Contrarywise, class *Anaerolineae* and its order *Caldilineales* (Phylum *Chloroflexi*) had a tendency to reduce their RAs throughout operation in the three biomass fractions analyzed (Fig. 2), although they were always more abundant on average in the attached biomass, particularly in the C4 samples (Fig. S6A, Fig. 4A), as already observed at the phylum level (Fig. 2). Other bacterial taxa which became enriched in the attached biomass compared to the suspended growth fraction were the Order *Nevskiales* (*Gammaproteobacteria*) and several families of the *Alphaproteobacteria* (*Hyphomicrobiaceae*, *Phyllobacteriaceae*, *Rhodobacteraceae*, *Rhodospirillaceae*) which reached higher RAs in the biomass sampled in either C1 or C4 than in the AS from August to October. In addition, a group of uncultured *Chloroflexi* was enriched in the C1 samples only (Fig. 2).

The OLR and NLR in the influent and the volatile biomass in the

bioreactor (MLVSS + BVFSS fractions) displayed very high positive correlations among them and are represented by a single vector marked as OLR in the plots of Fig. 4 and Fig. S6. In addition, these three variables correlated strong and negatively with both temperature (T) and SRT. According to BIOENV analysis (Table S11), higher RAs of the dominant classes *Betaproteobacteria* and *Gammaproteobacteria* (*Burkholderiales*, *Rhodocyclales*, unclassified *Betaproteobacteria* and *Xanthomonadales* at the order level) occurred with increasing availability of organic matter and N ($r > 0.70$), and consequently at lower T and shorter SRT ($r < -0.70$). The PLR in the influent only displayed strong positive correlations ($r > 0.70$) with the RA of the order *Rhodocyclales* and the group of unclassified *Betaproteobacteria*. The F/M ratio was represented by a very short vector in all the ordinations, indicating that its influence on the shaping of the bacterial community structure was weak.

The bacterial orders whose trends of RA showed more robust positive correlation coefficients with the %ORR were *Rhodocyclales* and *Rhodobacteriales* ($r = 0.97$ and $r = 0.76$ respectively, Table S11). %NRR was positively and robustly correlated with the RAs of *Hyphomicrobiales*, *Nevskiales*, *Rhodobacteriales*, *Rhodocyclales*, and *Rhodospirillales* ($r = 0.71$ – 0.99). %PRR was increased concomitantly with higher RAs of *Burkholderiales*, *Rhodocyclales*, *Xanthomonadales* and the group of unclassified *Betaproteobacteria* ($r = 0.7$ – 0.97). The families showing the strongest positive correlations ($r > 0.9$) with the efficiency of removal of both organic matter and nutrients were *Azonexaceae* ($r > 0.9$ with %ORR, %NRR and %PRR), *Rhodocyclaceae* ($r > 0.9$ with %ORR and %PRR), *Saprosiraceae* ($r = 0.87$ with %ORR and $r = 0.98$ with %PRR) and the group of unclassified *Burkholderiales* ($r = 0.9$ with %ORR and $r = 0.88$ with %PRR). Strong positive correlations ($r > 0.7$) among the RAs of the families *Hyphomicrobiaceae* and *Rhodobacteraceae* and the removal of N were already observed in previous experiments when the A²O was operated under the conventional configuration (Gallardo-Altamirano et al., 2019). Remarkably, in the present study, it was observed that in all the ordinations the %NRR increases in the direction of the C1 and C4 samples retrieved from August to October, indicating a closer link of the efficiency of the removal of this nutrient with the shifts of microbial communities experienced by the attached biomass fraction.

Fig. 4 also displays the MDS ordination based on the RAs of the PHYs identified at the genus level which reached $\geq 0.5\%$ RA in at least one sample, and the Pearson's product moment correlations among the vectors representing their trends of RA and those of the operational parameters and the removal efficiencies of organic matter, N and P are summarized in Table S11D. Regarding the efficiency of N removal, the genera *Bosea*, *Devosia*, *Hyphomicrobium* and *Rhodoplanes* showed moderate-to-high positive correlations with %NRR ($r = 0.63$ – 1.00 , Table S11D). These four genera accounted for 65–85% of the Illumina reads that were annotated as *Hyphomicrobiales*, the only among the top 5 more abundant orders which showed a high positive correlation with %NRR ($r = 0.82$, Table S11B). Other genera that correlated strongly with %NRR ($r > 0.85$) were *Dechloromonas* (*Rhodocyclales*), *Rhodobacter* (*Rhodobacteriales*), *Rubrivivax* (*Burkholderiales*) and *Sulfuritalea* (*Nitrosomonadales*). Remarkably, all of the aforementioned genera are described as denitrifiers (Falk et al., 2010; Magnusson et al., 1998; Marcondes de Souza et al., 2014; McIlroy et al., 2016; Nagashima et al., 2011; Oren and Xu, 2014; Pujalte et al., 2013) and reached higher average RAs in the attached biomass of the A²O-IFAS than in the suspended growth fraction, particularly in the C1 samples (Fig. S5). *Rhodobacter*, *Rubrivivax*, and *Sulfuritalea* were also identified among the dominant denitrifiers in previous studies in two A²O-IFAS full-scale plants (Phanwilai et al., 2020), and active denitrification by *Dechloromonas* and *Sulfuritalea* was demonstrated in a full-scale enhanced biological P removal plant by McIlroy et al. (2016).

The abovementioned results are in agreement with those of Lou et al. (2022), which found that after upgrading a full-scale A²O oxidation ditch by including carriers in all its sectors, the highest denitrification rates were connected to the colonization by heterotrophic denitrifiers of the biofilms at the front of the aerobic zone (closer to the anoxic area),

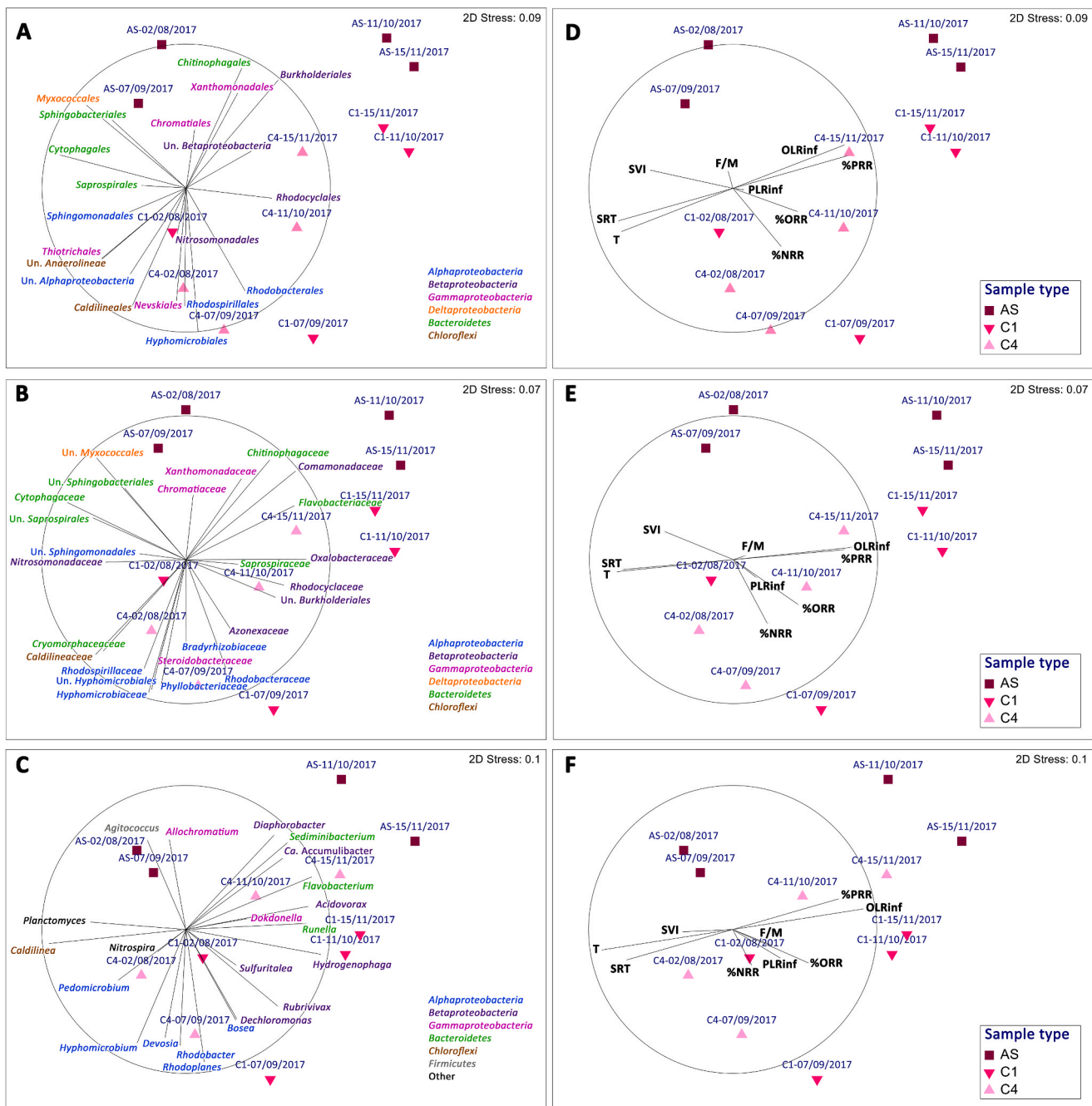


Fig. 4. Non-metric multidimensional scaling (MDS) plots, illustrating the ordinations of the samples retrieved from the suspended biomass in the activated sludge (AS) and attached biomass in C1 and C4 carriers of the anaerobic/anoxic/aerobic integrated fixed-film activated sludge (A²O-IFAS), according to the relative abundances of bacterial phylotypes identified by Illumina sequencing. In each plot, samples are represented on the ordination space with different symbols according to their type (AS, C1 or C4) and the sampling date is indicated. **A.** Ordination based on the relative abundance of *Bacteria* at the order level. **B.** Ordination based on the relative abundance of *Bacteria* at the family level. **C.** Ordination based on the relative abundance of *Bacteria* at the genus level. **D.** Correlations among operational parameters and the indicators of the efficiency of organic matter and nutrients' removal and the ordination shown in plot A. **E.** Correlations among operational parameters and the indicators of the efficiency of organic matter and nutrients' removal and the ordination shown in plot B. **F.** Correlations among operational parameters and the indicators of the efficiency of organic matter and nutrients' removal and the ordination shown in plot C. Vectors in plots A and B show the direction throughout the ordination of the relative abundances of bacterial orders and families with an average relative abundance $\geq 1\%$ in the set of samples. Vectors in plot C show the direction throughout the ordination of the relative abundances of bacterial genera with an average relative abundance $\geq 0.5\%$ in the set of samples. Taxa classified within the *Alpha*-, *Beta*-, *Gamma*- and *Deltaproteobacteria*, *Bacteroidetes* and *Chloroflexi* are shown using different colors. Vectors in plots D, E and F represent the direction throughout the ordination of the following variables: global food/microbial ratio (F/M), global solids retention time (SRT), organic loading rate of the influent (OLRinf), P loading rate of the influent (Pinf), sludge volumetric index (SVI), temperature (T), nitrogen removal rate (%NRR), organic removal rate (%ORR), P removal rate (%PRR). OLRinf, nitrogen loading rate in the influent (NLRinf) and the bioreactor biomass (MLSS + BFSS fractions) displayed very high positive correlations among them ($\rho > 0.9$), and are represented by a single vector in the plots. The stress level of the MDS plots (≤ 0.1) validates the 2D-representation of the biotic data distribution (Clarke and Warwick, 2001). Vectors with a length shorter than 0.2 had negligible influence on the ordination and are not shown. (For interpretation of the references to color in this figure legend, the reader is referred to the Web version of this article.)

while nitrifiers were enriched in further areas of the aerobic zone, where carriers were visibly less colonized, as also observed in the present study when comparing C1 and C4 carriers (Fig. S1). Phanwilai et al. (2020) also reported that the absolute abundances of both nitrifiers and heterotrophic denitrifiers measured by qPCR were significantly higher in the attached biomass than in the suspended growth of two full-scale A²O-IFAS operated at SRT = 7.5 and 5.2 days, and Wang et al. (2021a) found higher relative abundances of denitrifiers (which included *Dechloromonas* and *Hyphomicrobium*) in the biofilms of a pilot-scale IFAS-membrane bioreactor, compared to the AS fraction.

Several authors highlighted that the main advantage offered by IFAS for an enhanced N and P removal performance is to enable an increased residence time for the slow-growing nitrifiers by colonizing the carrier media, while the faster growing heterotrophs would mostly thrive in the suspended growth fraction (Onnis-Hayden et al., 2011; Waqas et al., 2020). In this sense, Zhao and Bai (2022) reported increased N-NH₄⁺ removal in an A²O when comparing the conventional and IFAS configurations (89.8% vs. 98.0%), concluding that the observed improvement was correlated with a higher RA of the nitrifying bacteria (particularly *Nitrospira*) in the attached biomass fraction. In the present study, the RAs of the *Nitrosomonadaceae* and *Nitrospira* tended to increase in the C4 samples (Figs. S4 and S5); however, no robust correlations were found among the RAs of these taxa and the %NRR (Fig. 4, Tables S11C and D). It must be taken into consideration that Zhao and Bai (2022) operated the A²O-IFAS using a much longer SRT (15 days) and higher MLSS concentrations (2430–3760 mg L⁻¹), also detecting much higher RAs of nitrifiers than those reported here. As previously stated, the average % NRR in the A²O-IFAS was significantly higher compared to the conventional A²O configuration used in the same pilot-scale plant in previous work, even though a shorter SRT was selected (Gallardo-Altamirano et al., 2021b); however, the N-NH₄⁺ removal rates were similarly high (>95%) in the three experimental phases (Table S1). The data presented here support that the incorporation of carriers enhanced the N removal performance by favoring an increase of the RAs of particular genera of denitrifiers in the attached biomass of C1 chamber of the aerobic bioreactor, rather than by boosting colonization by nitrifiers, under the operational conditions tested.

Two well-known phosphate accumulating (PAO) genera, *Dechloromonas* (*Rhodocyclales*) and *Ca. Accumulibacter* (Un. *Betaproteobacteria*) were identified in the A²O-IFAS samples. They were regarded as well as the major PAOs in other studies analyzing the diversity of IFAS systems (Wang et al., 2021a; Zhao and Bai, 2022). Both genera tended to increase their RAs in all the samples towards the end of the experiment, but while *Dechloromonas* was on average more abundant in the attached biomass, *Ca. Accumulibacter* became enriched in the AS (Fig. S5). This different niche preference is likely related to the ability of *Dechloromonas* spp. to denitrify (Petriglieri et al., 2021). Suspended growth is more often preferred by non-denitrifying PAO over the biofilm lifestyle in WWT plants, since these organisms require alternating aerobic and anaerobic conditions for their metabolism, and these are provided by the circulating mixed liquor of activated sludge in enhanced biological P removal (EBPR) systems such as the A²O-IFAS tested in this work (Onnis-Hayden et al., 2011).

Of the two PAO identified at the genus level, only *Ca. Accumulibacter* displayed a strong positive correlation with %PRR ($r = 0.94$, Table S11D). Its RA was favored at lower temperatures and shorter SRT, which were concomitant with the increase of ORL (Fig. 4). Remarkably, several other taxa at the family and genus level displayed robust positive correlations with %PRR (Tables S11C and D). Among these, *Rhodocyclaceae* have been widely reported to include PAO organisms (Goel and Motlagh, 2014; Klein et al., 2022), and *Comamonadaceae* were identified as key PAO coexisting with *Ca. Accumulibacter* in a sequencing batch reactor treating high-strength wastewater and operated at SRT shorter than 4 days (Ge et al., 2015). The role of the genus *Hydrogenophaga* in P removal in pilot-scale MBBR plants has been hinted in some studies (Iannacone et al., 2020, 2021), although to the best of the authors'

knowledge, its ability to accumulate polyphosphate in WWT plants has not been experimentally demonstrated to date. Thus, additional bacterial populations could be also contributing to P removal in the A²O-IFAS, either by storing polyphosphates, or providing substrates for PAO.

3.5. Linking the population dynamics of Bacteria and Archaea to the operational parameters and performance in the two-stage MAD

Fig. 5 and Fig. S7 show the MDS ordinations based on the RAs of the PHYs identified at the family and genus level of both *Bacteria* and *Archaea* in the two-stage MAD samples, and Table S12 displays the Pearson's product moment correlations among the vectors representing their trends of RA and those of the operational parameters and indicators of methanogenesis efficiency.

Taking all the samples altogether, *Rikenellaceae* had the highest average RAs in both the AcD and the MD (Fig. S4), although *Comamonadaceae* and *Paludibacteraceae* were also prevalent taxa in the AcD, with the three families cumulatively comprising 26.5–42.8% of the bacterial community. *Comamonadaceae* and *Paludibacteraceae* displayed robust positive correlations with the VFA/Alk ratio ($r > 0.80$) and correlated negatively with CH₄ recovery rate and %CH₄ in the biogas ($r = -0.69$ to -0.97). At both family and genus levels, the RAs of several taxa which were also enriched in the AcD compared to the MD (Figs. S4 and S5) displayed similar trends of correlation with the abovementioned variables (*Christensenellaceae*, *Lachnospiraceae*, *Rhodocyclaceae*, *Saprospiraceae*, Unclassified. *Burkholderiales*, and Unclassified *Eubacteriales*; *Dechloromonas*, *Ca. Accumulibacter*, *Diaphorobacter*, *Fusibacter*, *Microvirgula*, *Paludibacter*, *Proteiniclasticum*, *Rhodobacter*, and *Streptococcus*). Most of these taxa tended also to increase their RAs at higher values of OLR (Table S12). These patterns are consistent with the successful separation of acidogenesis in the first phase of the two-stage MAD, promoting a more efficient conversion of organic matter to VFAs while keeping methanogenesis low (Gallardo-Altamirano et al., 2021a). Interestingly, the populations which increased their RAs with the gradual lowering of temperature (35–30 °C) experienced in the AcD towards the end of the experiment were also correlated with a higher accumulation of VFAs.

In the MD, *Rikenellaceae* alone comprised 34.6–54.2% of the sequence reads in the samples (Fig. S4), and nearly 100% of the PHYs were identified to the genus level as belonging to the Blvii28 wastewater-sludge group (Fig. S5), of which the species *Acetobacteroides hydrogenigenes* is the only cultivated representative (Su et al., 2014). These bacteria are described as strictly anaerobic, carbohydrate fermenting organisms, which generate acetate, CO₂ and H₂ as end products, thus providing substrates for both hydrogenotrophic and acetoclastic methanogens, and have been often found dominant in mesophilic anaerobic digesters (Khan et al., 2021; Yu et al., 2022). The RAs of *Rikenellaceae* and *Acetobacteroides* (Blvii28) correlated positively with the CH₄ recovery rate and %CH₄ in the biogas, supporting the relevance of their role for an efficient methanogenesis (Fig. 5, Tables S12A and C). Other taxa showing similar trends of correlation in the MD although reaching considerably lower RAs in the sludge communities were the families *Anaerolineaceae*, *Chromatiaceae*, and *Synergistaceae*, and the genera *Allochromatium*, *Coprothermobacter*, *Kosmotoga*, *Syntrophomonas*, and *Thermoanaerovibrio* (Fig. 5). Species of all the aforementioned genera are described to produce H₂ as end-product of their metabolisms, and several of them are known to establish syntrophic associations with hydrogenotrophic methanogens (Chovatia et al., 2009; Dipippo et al., 2009; McInerney et al., 2008; Nie et al., 2021; Wang et al., 2021b). These symbioses among H₂ producers and consumers are regarded essential to assure efficient and stable operation of anaerobic digesters (Carballa et al., 2015).

The methanogenic community of both digesters was always >90% composed of hydrogenotrophic genera. In both digesters, the community was initially dominated by the family *Methanoregulaceae* and its genus *Methanolinea*; however, significant populations shifts were

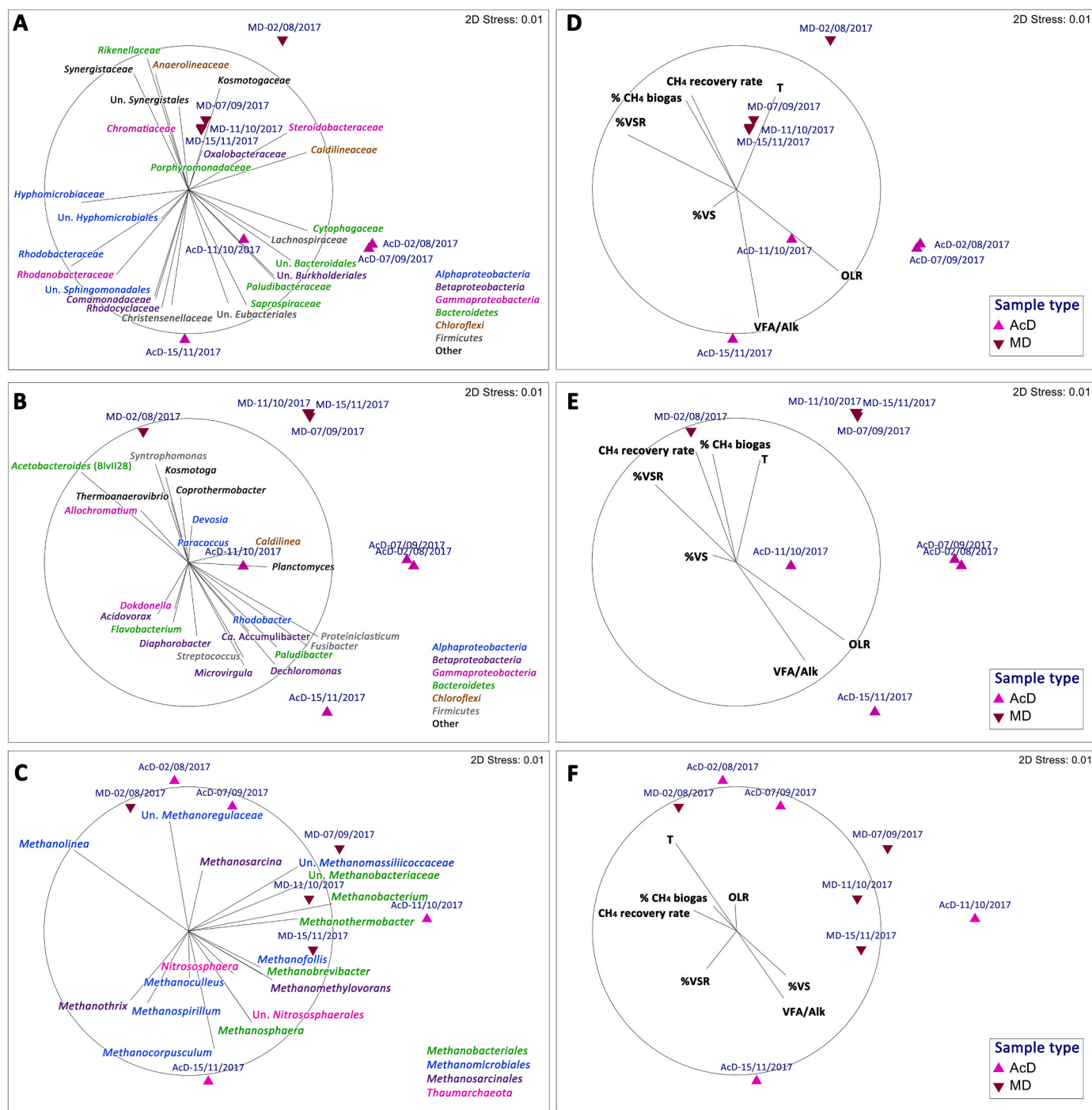


Fig. 5. Non-metric multidimensional scaling (MDS) plots, illustrating the ordinations of the samples retrieved from the effluents of the acidogenic and methanogenic digesters (AcD and MD) of the two-stage mesophilic anaerobic digestion (MAD) system, according to the relative abundances of bacterial and archaeal phylogenotypes identified by Illumina sequencing. In each plot, samples are represented on the ordination space with different symbols according to their type (AcD or MD) and the sampling date is indicated. **A.** Ordination based on the relative abundance of *Bacteria* at the family level. **B.** Ordination based on the relative abundance of *Bacteria* at the genus level. **C.** Ordination based on the relative abundance of *Archaea* at the genus level. **D.** Correlations among operational parameters and indicators of the efficiency of methanogenesis and the ordination shown in plot A. **E.** Correlations among operational parameters and indicators of the efficiency of methanogenesis and the ordination shown in plot C. Vectors in plots A show the direction throughout the ordination of the relative abundances of bacterial families with an average relative abundance $\geq 1\%$ in the set of samples. Vectors in plot B show the direction throughout the ordination of the relative abundances of bacterial genera with an average relative abundance $\geq 0.5\%$ in the set of samples. Vectors in plot C show the direction throughout the ordination of the relative abundances of all archaeal genera in the set of samples. Bacterial taxa classified within the *Alpha*-, *Beta*-, and *Gammaproteobacteria*, *Bacteroidetes*, *Chloroflexi* and *Firmicutes*, and archaeal taxa classified within the *Methanobacteriales*, *Methanomicrobiales*, *Methanosarcinales* and *Thaumarchaeota* are shown using different colors. Vectors in plots D, E and F represent the direction throughout the ordination of the following variables: %CH₄ in biogas, CH₄ recovery rate, temperature (T), volatile solids/total solids percentage (%VS/TS), volatile fatty acids to alkalinity ratio (VFA/Alk), organic loading rate (OLR), and % of volatile solids removal (%VSR). The stress level of the MDS plots (≤ 0.1) validates the 2D-representation of the biotic data distribution (Clarke and Warwick, 2001). Vectors with a length shorter than 0.2 had negligible influence on the ordination and are not shown. (For interpretation of the references to color in this figure legend, the reader is referred to the Web version of this article.)

observed in the October and November samplings, particularly in the AcD (Fig. 3). The RAs of the families *Methanobacteriaceae*, *Methanocorpusculaceae*, *Methanomicrobiaceae*, *Methanospirillaceae* and *Methanotrichaceae* tended to increase towards the end of the experiment. According to BIO-ENV analysis, *Methanobacteriaceae*, *Methanocorpusculaceae*, and *Methanomicrobiaceae* were enriched at lower temperatures and higher VFS/Alk ratios (Fig. S7, Table S12B), following trends opposed to those of the *Methanoregulaceae*. At the genus level, *Methanolinea* was displaced by *Methanocorpusculum* (*Methanocorpusculaceae*) (Fig. 3) and their RAs were influenced in opposite ways by the temperature and the available ORL (Fig. 5, Table S12). *Methanobacterium* (*Methanobacteriaceae*) increased their RAs throughout operation, but the correlations among the RA of this genus and the operating factors were negligible (Table S12D). *Methanolinea* was the only genus for which a robust positive correlation ($r > 0.98$) was observed among the increase of its RA and both the CH₄ recovery rate and %CH₄ in the biogas. A higher %VSR was observed with increasing RAs of both *Methanospirillum* and the acetotrophic specialist *Methanotrix*.

Overall, the prokaryotic community structure in the two-stage MAD and the correlations observed among the populations' dynamics and the efficiency of the acidogenesis and methanogenesis agreed with the results reported previously when the plant was operated with the same SRTs but fed with the PS and WAS of the A²O lacking the IFAS configuration (Gallardo-Altamirano et al., 2021a). Remarkably, in both studies robust positive correlations with %VSR and CH₄ recovery rate in the MD were detected for the *Rikenellaceae*, which were further identified here to the genus level as *Acetobacteroides* (Blvii28 wastewater-sludge group), providing a stronger support to the hypothesis of a major role of these organisms in the generation of substrates for methanogenesis. However, some interesting differences were also found. For instance, some of the taxa found prevalent in the AcD in the previous study were not detected here, and vice-versa (ie. *Xanthomonadaceae* compared to *Paludibacteraceae*). Also, in previous work a heavy enrichment with a single genus (*Methanolinea*, 70–92% RA) was observed throughout long-term operation, particularly in the AcD (Gallardo-Altamirano et al., 2021a), while in the present study several genera of methanogens codominated in the AcD, and population succession occurred mostly correlated to the temperature shift experienced in the AcD by the end of the experiment (Figs. 3 and 5). In previous work, Shaw et al., (2019) conducted microbial network analyses which predicted a displacement of *Methanoregulaceae* by *Methanospirillaceae* and *Methanomicrobiaceae* in a mesophilic laboratory-scale anaerobic digester under analogous temperature disturbances.

4. Conclusions

The improvement of the efficiency of nutrient removal in the pilot-scale A²O following an upgrade to the IFAS configuration significantly correlated with the shifts of RA of specific populations within the prokaryotic communities. Under the short SRT (5 days) operating conditions tested, both nitrifiers (*Nitrosomonadaceae*, *Nitrospira*, *Nitrososphaera*) and denitrifiers (*Bosea*, *Dechloromonas*, *Devosia*, *Hyphomicrobium*, *Rhodobacter*, *Rhodoplanes*, *Rubrivivax*, and *Sulfuritalea*) were enriched in the attached versus the suspended biomass fraction in the A²O, but only the increase of the RA of denitrifiers correlated strongly to %NRR. An increased %PRR was concomitant with the enrichment of *Ca. Accumulibacter* in the suspended biomass, although links with other genera potentially involved in P removal were also observed. Besides enabling efficient N and P removals in the A²O-IFAS, short SRT also contributed to generate a highly biodegradable WAS, which increased the absolute abundances of *Bacteria* and *Archaea* in the two-stage MAD and improved biogas and methane yields. Sludge retention time (SRT), together with carriers' addition, are easy adjustment variables for an optimization of this technology. In addition, bacteria of the *Rikenellaceae*, particularly *Acetobacteroides* (Blvii20 wastewater group), were

pointed as the key providers of substrates for methanogens in the two-stage MAD treating PS and WAS from either the conventional A²O or A²O-IFAS, and are potential microbial indicators of efficient performance in MAD processes.

Credit author statement

P. Maza-Márquez: Conceptualization, Investigation, Formal analysis, Visualization, Writing – review & editing. **M.J. Gallardo-Altamirano:** Conceptualization, Investigation, Formal analysis, Visualization, Writing – original draft, Writing – review & editing. **F. Osorio:** Conceptualization, Project administration, Funding acquisition. **C. Pozo:** Conceptualization, Writing – original draft, Writing – review & editing, Project administration, Funding acquisition, Supervision. **B. Rodelas:** Formal analysis, Visualization, Writing – original draft, Writing – review & editing, Supervision.

Declaration of competing interest

The authors declare that they have no known competing financial interests or personal relationships that could have appeared to influence the work reported in this paper.

Data availability

Data will be made available on request.

Acknowledgements

This work was funded by Spanish Ministerio de Economía y Competitividad (MINECO) and Fondo Europeo de Desarrollo Regional (FEDER) (CTM 2014-60131-P). Junta de Andalucía (Plan Andaluz de Investigación, Desarrollo e Innovación, PAIDI 2020) and MINECO (FPI program, BES-2015-073595) are acknowledged for personal grants to P. Maza-Márquez and M.J. Gallardo-Altamirano, respectively. The authors also wish to thank the Regional Government of Murcia, Spain (ESAMUR) and Murcia Water Works (EMUASA) for their collaboration in this research project and provision of facilities at Murcia Este Wastewater Treatment Plant (Murcia, Spain). Funding for open access charge: Universidad de Granada / CBUA.

Appendix A. Supplementary data

Supplementary data to this article can be found online at <https://doi.org/10.1016/j.chemosphere.2023.139164>.

References

- Appels, L., Baeyens, J., Degreè, J., Dewil, R., 2008. Principles and potential of the anaerobic digestion of waste-activated sludge. *Prog. Energy Combust. Sci.* 34, 755–781. <https://doi.org/10.1016/j.pecs.2008.06.002>.
- Aqeel, H., Liss, S.N., 2022. Fate of sloughed biomass in integrated fixed-film systems. *PLoS One* 17, e0262603. <https://doi.org/10.1371/journal.pone.0262603>.
- Bolzonella, D., Pavan, P., Battistoni, P., Cecchi, F., 2005. Mesophilic anaerobic digestion of waste activated sludge: influence of the solid retention time in the wastewater treatment process. *Process Biochem.* 40, 1453–1460. <https://doi.org/10.1016/j.procbio.2004.06.036>.
- Caporaso, J.G., Lauber, C.L., Walters, W.A., Berg-lyons, D., Huntley, J., Fierer, N., Owens, S.M., Betley, J., Fraser, L., Bauer, M., Gormley, N., Gilbert, J.A., Smith, G., Knight, R., 2012. Ultra-high-throughput microbial community analysis on the Illumina HiSeq and MiSeq platforms. *ISME J.* 6, 1621–1624. <https://doi.org/10.1038/ismej.2012.8>.
- Carballa, M., Regueiro, L., Lema, J.M., 2015. Microbial management of anaerobic digestion: exploiting the microbiome-functionality nexus. *Cur. Op. Biotechnol.* 33, 103–111. <https://doi.org/10.1016/j.copbio.2015.01.008>.
- Chae, K.J., Jang, A., Yim, S.K., Kim, I.S., 2008. The effects of digestion temperature and temperature shock on the biogas yields from the mesophilic anaerobic digestion of swine manure. *Bioresour. Technol.* 99, 1–6. <https://doi.org/10.1016/j.biortech.2006.11.06>.
- Chovatia, M., Sikorski, J., Schröder, M., Lapidus, A., Nolan, M., Tice, H., Glavina Del Rio, T., Copeland, A., Cheng, J.F., Lucas, S., Chen, F., Bruce, D., Goodwin, L.,

- Pitluck, S., Ivanova, N., Mavromatis, K., Ovchinnikova, G., Pati, A., Chen, A., Palaniappan, K., Land, M., Hauser, L., Chang, Y.J., Jeffries, C.D., Chain, P., Saunders, E., Detter, J.C., Brettin, T., Rohde, M., Göker, M., Spring, S., Bristow, J., Markowitz, V., Hugenholtz, P., Kyripides, N.C., Klenk, H.P., Eisen, J.A., 2009. Complete genome sequence of *Thermaerovibrio acidaminovorans* type strain (Su883). *Stand. Genomic. Sci.* 1, 254–261. <https://doi.org/10.4056/signs.40645>.
- Demir, S., 2020. Comparison of performances of biological nutrient removal systems for municipal wastewater treatment. *Sigma J. Eng. Nat. Sci.* 38, 1235–1248.
- Dipippo, J.L., Nesbø, C.L., Dahle, H., Doolittle, W.F., Birkland, N.K., Noll, K.M., 2009. *Kosmotoga olearia* gen. nov., sp. nov., a thermophilic, anaerobic heterotroph isolated from an oil production fluid. *Int. Journal Sys. Evol. Microbiol.* 59, 2991–3000. <https://doi.org/10.1099/ijs.0.008045-0>.
- Falk, S., Liu, B., Braker, G., 2010. Isolation, genetic and functional characterization of novel soil *nirK*-type denitrifiers. *Syst. Appl. Microbiol.* 33, 337–347. <https://doi.org/10.1016/j.syapm.2010.06.004>.
- Fan, L., McElroy, K., Thomas, T., 2012. Reconstruction of ribosomal RNA genes from metagenomic data. *PLoS One* 7, e39948. <https://doi.org/10.1371/journal.pone.0039948>.
- Ferrera, I., Sánchez, O., 2016. Insights into microbial diversity in wastewater treatment systems: how far have we come? *Biotechnol. Adv.* 34, 790–802. <https://doi.org/10.1016/j.biotechadv.2016.04.003>.
- Gallardo-Altamirano, M.J., Maza-Márquez, P., Peña-Herrera, J.M.M., Rodelas, B., Osorio, F., Pozo, C., 2018. Removal of anti-inflammatory/analgesic pharmaceuticals from urban wastewater in a pilot-scale A²O system: linking performance and microbial population dynamics to operating variables. *Sci. Total Environ.* 643, 1481–1492. <https://doi.org/10.1016/j.scitotenv.2018.06.284>.
- Gallardo-Altamirano, M.J., Maza-Márquez, P., Montemurro, N., Rodelas, B., Osorio, F., Pozo, C., 2019. Linking microbial diversity and population dynamics to the removal efficiency of pharmaceutically active compounds (PhACs) in an anaerobic/anoxic/aerobic (A²O) system. *Chemosphere* 233, 828–842. <https://doi.org/10.1016/j.chemosphere.2019.06.017>.
- Gallardo-Altamirano, M.J., Maza-Márquez, P., Montemurro, N., Pérez, S., Rodelas, B., Osorio, F., Pozo, C., 2021a. Insights into the removal of pharmaceutically active compounds from sewage sludge by two-stage mesophilic anaerobic digestion. *Sci. Total Environ.* 789, 147869 <https://doi.org/10.1016/j.scitotenv.2021.147869>.
- Gallardo-Altamirano, M.J., Maza-Márquez, P., Pérez, S., Rodelas, B., Pozo, C., Osorio, F., 2021b. Fate of pharmaceutically active compounds in a pilot-scale A²O integrated fixed-film activated sludge (IFAS) process treating municipal wastewater. *J. Environ. Chem. Eng.* 9, 105398 <https://doi.org/10.1016/j.jece.2021.105398>.
- Ge, H., Batstone, D.J., Keller, J., 2015. Biological phosphorus removal from abattoir wastewater at very short sludge ages mediated by novel PAO clade *Comamonadaceae*. *Water Res.* 69, 173–182. <https://doi.org/10.1016/j.watres.2014.11.026>.
- Goel, R.K., Motlagh, A.M., 2014. Biological phosphorus removal. In: *Ajta, S. (Ed.), Comprehensive Water Quality and Purification*. Elsevier, The Netherlands, pp. 150–162. <https://doi.org/10.1016/B978-0-12-382182-9.00051-7>.
- Gonzalez, A., Hendriks, A.T.W.M., van Lier, J.B., de Kreuk, M., 2018. Pre-treatments to enhance the biodegradability of waste activated sludge: elucidating the rate limiting step. *Biotechnol. Adv.* <https://doi.org/10.1016/j.biotechadv.2018.06.001>.
- Hammer, Ø., Harper, D.A.T., Ryan, P.D., 2001. *Past: paleontological statistics software package for education and data analysis*. *Palaeontol. Electron.* 4, 178.
- Hsieh, T.C., Ma, K.H., Chao, A., 2016. iNEXT: an R package for rarefaction and extrapolation of species diversity (Hill numbers). *Methods Ecol. Evol.* 7, 1451–1456. <https://doi.org/10.1111/2041-210X.12613>.
- Iannacone, F., Di Capua, F., Granata, F., Gargano, R., Esposito, G., 2020. Simultaneous nitrification, denitrification and phosphorus removal in a continuous-flow moving bed biofilm reactor alternating microaerobic and aerobic conditions. *Bioresour. Technol.* 310, 123453 <https://doi.org/10.1016/j.biortech.2020.123453>.
- Iannacone, F., Di Capua, F., Granata, F., Gargano, R., Esposito, G., 2021. Shortcut nitrification denitrification and biological phosphorus removal in acetate- and ethanol-fed moving bed biofilm reactors under microaerobic/aerobic conditions. *Bioresour. Technol.* 330, 124958 <https://doi.org/10.1016/j.biortech.2021.124958>.
- Jo, J., Price-Whelan, A., Dietrich, L.P.E., 2022. Gradients and consequences of heterogeneity in biofilms. *Nat. Rev. Microbiol.* 20, 593–607. <https://doi.org/10.1038/s41579-022-00692-2>.
- Khan, M.A., Khan, S.T., Sequeira, M.C., Faheem, S.M., Rais, N., 2021. Illumina sequencing of 16S rRNA genes reveals a unique microbial community in three anaerobic sludge digesters of Dubai. *PLoS One* 16, e0249023. <https://doi.org/10.1371/journal.pone.0249023>.
- Klein, E., Weiler, J., Wagner, M., Čeliković, M., Niemeyer, C.M., Horn, H., Gescher, J., 2022. Enrichment of phosphate-accumulating organisms (PAOs) in a microfluidic model biofilm system by mimicking a typical aerobic granular sludge feast/famine regime. *Appl. Microbiol. Biotechnol.* 106, 1313–1324. <https://doi.org/10.1007/s00253-022-11759-8>.
- Kwon, S., Taek-Seung, K., Gi Hyeon, Y., Joon-Hong, J., Hee-Deung, P., 2010. Bacterial community composition and diversity of a full-scale integrated fixed-film activated sludge system as investigated by pyrosequencing. *J. Microbiol. Biotechnol.* 20, 1717–1723. <https://doi.org/10.4014/jmb.1007.07012>.
- Lou, T., Peng, Z., Jiang, K., Niu, N., Wang, J., Liu, A., 2022. Nitrogen removal characteristics of biofilms in each area of a full-scale AAO oxidation ditch process. *Chemosphere* 302, 134871. <https://doi.org/10.1016/j.chemosphere.2022.134871>.
- Magnusson, G., Edin, H., Dalhammar, G., 1998. Characterization of efficient denitrifying bacteria strains isolated from activated sludge by 16S-rDNA analysis. *Water Sci. Technol.* 38, 63–68.
- Marcondes de Souza, J.A., Carareto Alves, L.M., de Mello Varani, A., de Macedo Lemos, E.G., 2014. The family bradyrhizobiaceae. In: *Rosemberg, E., de Long, E.F., Lory, S., Stackebrandt, E., Thompson, F. (Eds.), The Prokaryotes – Alphaproteobacteria and Betaproteobacteria*. Springer-Verlag, Berlin, pp. 135–154. https://doi.org/10.1007/978-3-642-30197-1_377.
- Maspolim, Y., Zhou, Y., Guo, C., Xiao, K., Ng, W.J., 2015. Determination of the archaeal and bacterial communities in two-phase and single-stage anaerobic systems by 454 pyrosequencing. *J. Environ. Sci. (China)* 36, 121–129. <https://doi.org/10.1016/j.jes.2015.02.017>.
- Maza-Márquez, P., Vilchez-Vargas, R., Kerckhof, F.M., Aranda, E., González-López, J., Rodelas, B., 2016. Community structure, population dynamics and diversity of fungi in a full-scale membrane bioreactor (MBR) for urban wastewater treatment. *Water Res.* 105, 507–519. <https://doi.org/10.1016/j.watres.2016.09.021>.
- McIlroy, S.J., Starnawska, A., Starnawski, P., Saunders, A.M., Nierychlo, M., Nielsen, P.H., Nielsen, J.L., 2016. Identification of active denitrifiers in full-scale nutrient removal wastewater treatment systems. *Environ. Microbiol.* 18, 50–64. <https://doi.org/10.1111/1462-2920.12614>.
- McInerney, M.J., Struchtemeyer, C.G., Sieber, J., Mouttaki, H., Stams, A.J., Schink, B., Rohlin, L., Gunsalus, R.P., 2008. Physiology, ecology, phylogeny, and genomics of microorganisms capable of syntrophic metabolism. *Ann. NY. Acad. Sci.* 1125, 58–72. <https://doi.org/10.1196/annals.1419.005>.
- Metcalf, Eddy, I., 2003. *Wastewater Engineering, Treatment and Reuse 4th Edition*, 4th ed. McGraw-Hill, New York.
- Nagashima, S., Shimada, K., Verméglio, A., Nagashima, K.V.P., 2011. The cytochrome *cg* involved in the nitrite reduction pathway acts also as electron donor to the photosynthetic reaction center in *Rubrivivax gelatinosus*. *Biochim. Biophys. Acta* 1807, 189–196.
- Nie, E., He, P.J., Duan, H., Zhang, H., Shao, L., Lü, F., 2021. Microbial and functional succession during anaerobic digestion along a fine-scale temperature gradient of 26–65 °C. *ACS Sustainable Chem. Eng.* 9, 15935–15945. <https://doi.org/10.1021/acscuschemeng.1c06023>.
- Onnis-Hayden, A., Majed, N., Schramm, A., Gu, A.Z., 2011. Process optimization by decoupled control of key microbial populations: distribution of activity and abundance of polyphosphate-accumulating organisms and nitrifying populations in a full-scale IFAS-EBPR plant. *Water Res.* 45, 3845–3854. <https://doi.org/10.1016/j.watres.2011.04.039>.
- Oren, A., Xu, X.W., 2014. The family Hyphomicrobiaceae. In: *Rosemberg, E., de Long, E.F., Lory, S., Stackebrandt, E., Thompson, F. (Eds.), The Prokaryotes – Alphaproteobacteria and Betaproteobacteria*. Springer-Verlag, pp. 248–281. https://doi.org/10.1007/978-3-642-30197-1_377.
- Parkin, G.F., Owen, W.F., 1986. Fundamentals of anaerobic digestion of wastewater sludges. *J. Environ. Eng. (United States)* 112, 867–920. [https://doi.org/10.1061/\(ASCE\)0733-9372\(1986\)112:5\(867\)](https://doi.org/10.1061/(ASCE)0733-9372(1986)112:5(867)).
- Petriglieri, F., Singleton, C., Peces, M., Petersen, J.F., Nierychlo, M., Nielsen, P.H., 2021. "Candidatus Dechloromonas phosphoritropha" and "Ca. D. phosphorivorans", novel polyphosphate accumulating organisms abundant in wastewater treatment systems. *ISME J.* 15, 3605–3614. <https://doi.org/10.1038/s41396-021-01029-2>.
- Phanwilai, S., Kangwannarakul, N., Noophan, P., Kasahara, T., Terada, A., Munakata-Marr, J., Figueroa, L.A., 2020. Nitrogen removal efficiencies and microbial communities in full-scale IFAS and MBBR municipal wastewater treatment plants at high COD:N ratio. *Front. Environ. Sci. Eng.* 14, 115. <https://doi.org/10.1007/s11783-020-1374-2>.
- Ponsá, S., Ferrer, I., Vázquez, F., Font, X., 2008. Optimization of the hydrolytic-acidogenic anaerobic digestion stage (55 °C) of sewage sludge: influence of pH and solid content. *Water Res.* 42, 3972–3980. <https://doi.org/10.1016/j.watres.2008.07.002>.
- Pujalte, M.J., Lucena, T., Ruvira, M.A., Ruiz Arahall, D., Maciá, M.C., 2013. The family Rhodobacteraceae. In: *Rosemberg, E., de Long, E.F., Lory, S., Stackebrandt, E., Thompson, F. (Eds.), The Prokaryotes – Alphaproteobacteria and Betaproteobacteria*. Springer-Verlag, pp. 440–512. https://doi.org/10.1007/978-3-642-30197-1_377.
- Raj, S.E., Banu, J.R., Kaliappan, S., Yeom, I.T., Kumar, S.A., 2013. Effects of side-stream, low temperature phosphorus recovery on the performance of anaerobic/anoxic/oxic systems integrated with sludge pretreatment. *Bioresour. Technol.* 140, 376–384. <https://doi.org/10.1016/j.biortech.2013.04.061>.
- Reboleiro-Rivas, P., Martín-Pascual, J., Morillo, J.A., Juárez-Jiménez, B., Poyatos, J.M., Rodelas, B., González-López, J., 2016. Interlinkages between bacterial populations dynamics and the operational parameters in a moving bed membrane bioreactor treating urban sewage. *Water Res.* 88, 796–807. <https://doi.org/10.1016/j.watres.2015.10.059>.
- Rodelas, B., 2021. Nitrogen cycle in wastewater treatment plants. In: *González-Martínez, A., González-López, J. (Eds.), Nitrogen Cycle: Ecology, Biotechnological Applications and Environmental Impacts*. CRC Press, pp. 144–202. <https://doi.org/10.1201/9780429291180>.
- Rosso, D., Lothman, S.E., Jeung, M.K., Pitt, P., Gellner, W.J., Stone, A.L., Howard, D., 2011. Oxygen transfer and uptake, nutrient removal, and energy footprint of parallel full-scale IFAS and activated sludge processes. *Water Res.* 45, 5987–5996. <https://doi.org/10.1016/j.watres.2011.08.060>.
- Shaw, G.T., Weng, C.Y., Chen, C.Y., Weng, F.C., Wang, D., 2019. A systematic approach re-analyzing the effects of temperature disturbance on the microbial community of mesophilic anaerobic digestion. *Sci. Rep.* 9, 6560. <https://doi.org/10.1038/s41598-019-42987-0>.
- Su, X.L., Tian, Q., Zhang, J., Yuan, X.Z., Shi, X.S., Guo, R.B., Qiu, Y.L., 2014. *Acetobacteroides hydrogenigenes* gen. nov., sp. nov., an anaerobic hydrogen-producing bacterium in the family *Rikenellaceae* isolated from a reed swamp. *Int. J. Syst. Evol. Microbiol.* 64, 2986–2991. <https://doi.org/10.1099/ijs.0.063917-0>.
- Urakawa, H., Bernhard, A.E., 2017. Wetland management using microbial indicators. *Ecol. Eng.* 108 (B), 456–476. <https://doi.org/10.1016/j.ecoleng.2017.07.022>.

- Verma, S., Kuila, A., Jacob, S., 2022. Role of biofilms in waste water treatment. *Appl. Biochem. Biotechnol.* <https://doi.org/10.1007/s12010-022-04163-5> (in press).
- Wang, X.L., Peng, Y.Z., Wang, S.Y., Fan, J., Cao, X.M., 2006. Influence of wastewater composition on nitrogen and phosphorus removal and process control in A²O process. *Bioproc. Biosyst. Eng.* 28, 397–404. <https://doi.org/10.1007/s00449-006-0044-5>.
- Wang, D., Tao, J., Fan, F., Xu, R., Meng, F., 2021a. A novel pilot-scale IFAS-MBR system with low aeration for municipal wastewater treatment: linkages between nutrient removal and core functional microbiota. *Sci. Total Environ.* 776, 145858 <https://doi.org/10.1016/j.scitotenv.2021.145858>.
- Wang, Y., Jing, Y., Lu, C., Kongjan, P., Wang, J., Awasthi, M.K., Tahir, N., Zhang, Q., 2021b. A syntrophic co-fermentation model for bio-hydrogen production. *J. Clean. Prod.* 317, 128288 <https://doi.org/10.1016/j.jclepro.2021.128288>.
- Waqas, S., Bilal, M.R., Man, Z., Wibisono, Y., Jaafar, J., Indra Mahlia, T.M., Khan, A.L., Aslam, M., 2020. Recent progress in integrated fixed-film activated sludge process for wastewater treatment: a review. *J. Environ. Manag.* 268, 110718 <https://doi.org/10.1016/j.jenvman.2020.110718>.
- Wu, B., Li, Y., Lim, W., Lee, S.L., Guo, Q., Fane, A.G., Liu, Y., 2017. Single-stage versus two-stage anaerobic fluidized bed bioreactors in treating municipal wastewater: performance, foulant characteristics, and microbial community. *Chemosphere* 171, 158–167. <https://doi.org/10.1016/j.chemosphere.2016.12.069>.
- Xia, Y., Wen, X., Zhang, B., Yang, Y., 2018. Diversity and assembly patterns of activated sludge microbial communities: a review. *Biotechnol. Adv.* 36, 1038–1047. <https://doi.org/10.1016/j.biotechadv.2018.03.005>.
- Xiao, K., Zhou, L., He, B., Qian, L., Wan, S., Qu, L., 2016. Nitrogen and phosphorus removal using fluidized-carriers in a full-scale A²O biofilm system. *Biochem. Eng. J.* 115, 47–55. <https://doi.org/10.1016/j.bej.2016.08.004>.
- Xu, Y., Lu, Y., Zheng, L., Wang, Z., Dai, X., 2020. Perspective on enhancing the anaerobic digestion of waste activated sludge. *J. Hazard Mater.* 389, 121–847. <https://doi.org/10.1016/j.jhazmat.2019.121847>.
- Yang, Y., Yu, K., Xia, Y., Lau, F.T.K., Tang, D.T.W., Fung, W.C., Fang, H.H.P., Zhang, T., 2014. Metagenomic analysis of sludge from full-scale anaerobic digesters operated in municipal wastewater treatment plants. *Appl. Microbiol. Biotechnol.* 98, 5709–5718. <https://doi.org/10.1007/s00253-014-5648-0>.
- Yu, N., Mou, A., Sun, H., Liu, Y., 2022. Anaerobic digestion of thickened waste activated sludge under calcium hypochlorite stress: performance stability and microbial communities. *Environ. Res.* 212 (Pt C), 113441 <https://doi.org/10.1016/j.envres.2022.113441>.
- Zhao, W., Bai, M., 2022. Upgrading integrated fixed-film activated sludge (IFAS) system into separated two-sludge denitrifying phosphorus removal system: nutrient removal and microbial structure. *Chemosphere* 307, 135918. <https://doi.org/10.1016/j.chemosphere.2022.135918>.